

Electron microscope study of dislocations introduced by deformation in a Si between 77 and 873 K

T. Okuno · H. Saka

Received: 1 April 2012 / Accepted: 3 September 2012 / Published online: 19 September 2012
© Springer Science+Business Media, LLC 2012

Abstract Dislocations were introduced into Si by scratching between 77 and 873 K. The nature and configurations of dislocations were determined by the weak-beam method. Dislocations introduced below 703 K were perfect dislocations of the shuffle set, while those introduced above 823 K were dissociated dislocations of the glide set. At 77 K, the shuffle set of dislocations was very straight; between RT and 363 K, the shuffle set of dislocations blunted, but mostly parallel to crystallographic orientations. Above 383 K, the shuffle set of dislocations was heavily zigzagged. The mechanism responsible for the zigzagging of the shuffle set of dislocations was discussed.

Introduction

Dislocations in diamond-structure Si can assume two sets of configurations, i.e., the shuffle (hereinafter denoted by SH) set and the glide (hereinafter denoted by GL) set [1]. The GL set of dislocations is activated above the ductile–brittle transition temperature, DBTT (800–930 K, depending on the strain rate and purity [2]), and has been studied very well [3–5]. It is now established that they are dissociated into two Shockley partials and aligned parallel to $\langle 110 \rangle$; the latter indicates that the Peierls valley for the GL set of dislocations is deep along $\langle 110 \rangle$ directions. In contrast, the SH set of dislocations is activated below DBTT under some special circumstances such as under a high pressure or under

indentation or scratch [6–8], but has been studied to a much lesser extent as compared with the GL set dislocations. Experimental results obtained so far about the SH set of dislocation can be summarized as follows [9]:

1. They are activated in Si by compression in a constrained state; the examples being compression in a high pressure cell, indentation, and scratching.
2. They are aligned along $\langle 110 \rangle$, $\langle 112 \rangle$, and $\langle 123 \rangle$.
3. They can be introduced at temperatures as low as 77 K [10].

Recently, three interesting studies concerning dislocation behavior in Si have been reported. One is the observation of increase in fracture toughness of Si thin crystals at around 250–373 K [12]. The second is the occurrence of the SH set of dislocation in a Si device rapidly heated to 1173 K [13], and the last is the observation of a weakly dissociated dislocation deformed at 373 K [14]. This rekindles interest in studying dislocations above room temperature in Si in more detail.

Nomenclature

Si crystallizes in the diamond cubic structure, which corresponds to two interpenetrating fcc lattices, one of which is displaced by $(1/4, 1/4, 1/4)$ with respect to the other. The slip system is $\frac{1}{2} \langle 110 \rangle / \{111\}$ as in the case of other fcc structures. The $\{111\}$ planes in the diamond structure contain the sequence AaBbCcAaBbCc, as shown in Fig. 1. There are two possibilities as to the position of the slip plane $\{111\}$. If the slip plane is between c and A (or equivalently, a and B or b and C), as indicated by GL in Fig. 1, the dislocation belongs to the GL set of dislocations. On the other hand, if the slip plane lies between C

T. Okuno · H. Saka (✉)
Nagoya University, Nagoya 464-8603, Japan
e-mail: saka@nagoya-u.jp

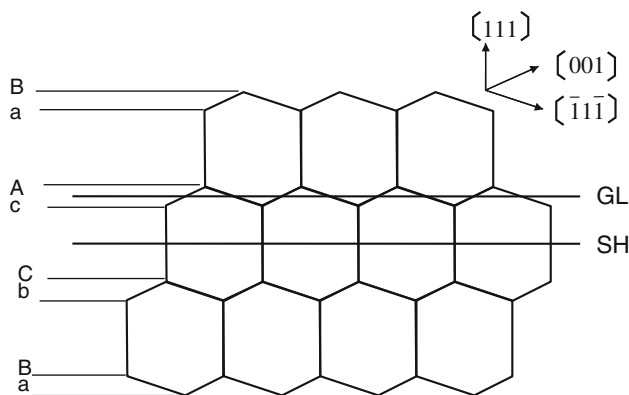


Fig. 1 The diamond structure as viewed along the $[1\bar{1}0]$ direction

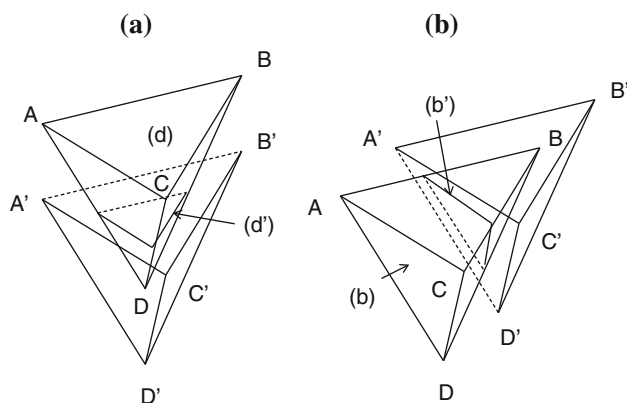


Fig. 2 Thompson's tetrahedron for GL set and SH set of dislocations. **a** For dislocations lying on (d) or (d') . **b** For dislocations lying on (c) or (c')

and c (or equivalently, B and b or A and a), as indicated by SH in Fig. 1, the dislocation belongs to the SH set of dislocations. To distinguish between the two sets of dislocations with identical Burgers vectors, double Thompson tetrahedra can be used, as shown in Fig. 2 [1]. Here, the SH set of dislocations lies on the tetrahedron $A'B'C'D'$, whereas the GL set of dislocations lies on $ABCD$. Figure 2a, b correspond to the case where the slip plane is $ABC(d)$ [or $A'B'C(d')$] and the case of slip plane of $ACD(c)$ [or $A'C'D'(c')$]. Thus, if a dislocation of the GL set on (d) plane has a Burgers vector of, say, AC , the corresponding dislocation of the SH set has the Burgers vector of $A'B'$ lying on (d') . If the dislocation with Burgers vector of AC of the GL set lies on (b) plane instead, the corresponding dislocation of the SH set has the Burgers vector of $A'B'$ lying on (b') , and so on.

Experimental procedures

Materials and introduction of dislocations

Two types of Si were used: B doped CZ-Si (~ 10 ohm.cm, $O_i = 1.2 \times 10^{18}$ atoms/cm³) donated by Mitsubishi Materials Corp. and an intrinsic Si wafer (>8400 ohm.cm) purchased from University Wafer Corp. Both of them were $\langle 100 \rangle$ orientated wafers about 0.2 mm in thickness. Most of the experiments were carried out on the CZ-Si, which was scratched with a diamond stylus along $[110]$ direction with a load of a few grams at a rate of 5 cm/s in a temperature range between 77 and 873 K (Fig. 3a). The intrinsic Si was deformed in a similar way at 623 K. Except at 77 K, where the sample was immersed in liquid nitrogen, the scratching was performed in air. It has been established that the features of those dislocations introduced by scratching are essentially similar to those obtained under a confining pressure [15].

TEM observations

Thin foil specimens were prepared in a JEOL FIB operated at 30 kV in such a way that the foil is either perpendicular or slightly inclined to the scratching. The surface orientation of the former is $[110]$ and the latter is $[111]$. The general geometry is shown in Fig. 3a. Here, $[110]$ (or equivalently, DC in the Thompson's tetrahedron) corresponds to the direction of scratching. Figure 3b shows the stereograph of the specimen with the surface orientation of $[110]$. These specimens were examined both in the conventional bright-field imaging mode and in the weak-beam method in a Hitachi H-800 microscope operated at an accelerating voltage of 200 kV. Some of them were examined in a high-voltage electron microscope RS HVEM 1000 [16] equipped with a high-angle tilting device, operated at an accelerating voltage of 1MV, to obtain three-dimensional information. In addition to dislocations, a variety of defects such as cracks and twins were introduced by scratching. Those dislocations suspected of being affected by nearby cracks were neglected.

Heat treatment before and after introduction of dislocations

Some specimens were subject to two types of heat treatment as shown in the following.

1. Deformed at T_d , followed by annealing at T_a (in foil or in bulk) ($T_d < T_a$).
2. Annealed at T'_a , followed by deformation at T'_d ($T'_a > T'_d$).

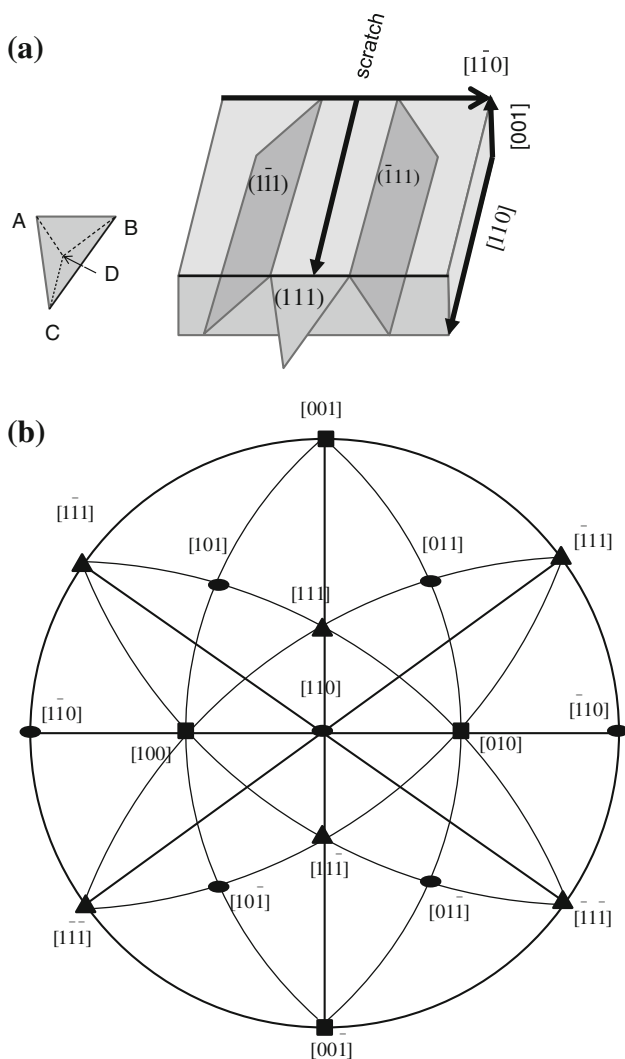


Fig. 3 **a** Geometry of specimen. **b** Stereo projection for orientation [110]

Results

As-introduced dislocations in CZ-Si

Between 77 K and RT

Figure 4a, b show dislocations introduced at liquid nitrogen temperature imaged in the weak-beam method. The direction of the incident beam, B, is [110], i.e., CD in the Thompson’s tetrahedron.¹ The triangle A, B,C,D (below) corresponds to the Thompson’s tetrahedron projected along B. The suffix *pr* indicates that the relevant straight line corresponds to the projection of the crystallographic

¹ Strictly speaking, A, B, C, and D should be used for the GL set and A', B', C', and D' for the SH set; however, hereinafter, A, B, C, and D in the inset stand for both A, B, C, and D and A', B', C', and D'.

direction to which the suffix *pr* is attached. For example, [132]_{pr} stands for the projection of the [132] direction along B = [110], i.e., on the (110) plane. The dislocations are very long and straight, aligning along <110>, <112>, and <123> directions with sharp bends. A comprehensive contrast experiment was carried out. There was no evidence of dissociation into two Shockley partials, at least within the resolution limit of the weak-beam method. Therefore, it is reasonable to conclude that the dislocations were not dissociated, but perfect dislocations. These results are in good agreement with the previous observations on dislocations introduced by indentation [10, 11].

Figure 5 shows dislocations introduced at room temperature. Dislocations are aligned approximately along <112> and <123> directions. However, they are much less straight and the bends are less sharp than at 77 K. This is in good agreement with the previous observation [6, 10].

Between 363 and 703 K

This tendency of the dislocation to become less straight increased on further increasing the deformation temperature. Figure 6 shows dislocations introduced at 363 K. While some segments of dislocations are aligned approximately along <112> and <123> directions, as indicated by ①, ②, ③, and ④, they are not very straight, and the bends are blunt, being rather smoothly curved. There is some evidence that pinning points are distributed along the dislocations as indicated by arrows. Essentially, similar features were obtained at 383 K.

Figure 7 shows dislocations introduced at 403 K. Four dislocations are imaged. Dislocations ①, ②, ③ are rather straight and smoothly curved. In contrast, dislocation ④ is zigzagged heavily. These dislocations ①, ②, ③ most likely lie on (111) plane; then, the possible (total) Burgers vectors should be one of AB, BC, and CA. Since these dislocations are out of contrast under $g = \bar{1}11(c)$, the Burgers vector must be AC (or CA). Similarly, dislocation ④ disappears under $g = 1\bar{1}\bar{1}$ (a) and $\bar{1}\bar{1}\bar{1}$ (b). Therefore, the Burgers vector must be BC (or CB). The dislocation ④ makes an angle of 60° with respect to its Burgers vector (BC) as a whole. But, it is too heavily zigzagged for each of the segments comprising dislocation ④ to be taken as aligning along any crystallographic directions.

Figure 8a and b show dislocations introduced at 472 K. Some dislocations, shown in Fig. 8a or dislocations ① and ② shown in Fig. 8b, are approximately aligned along <110>, <112>, and <123>, while others, such as dislocations ③ and ④ shown in Fig. 8b, are zigzagged heavily.

Figure 9 shows dislocation introduced at 623 K. In Fig. 9a, dislocations lying on a (111) plane are viewed from the top, that is, with the electron beam direction B being B = [110]; it is clear that dislocations are heavily

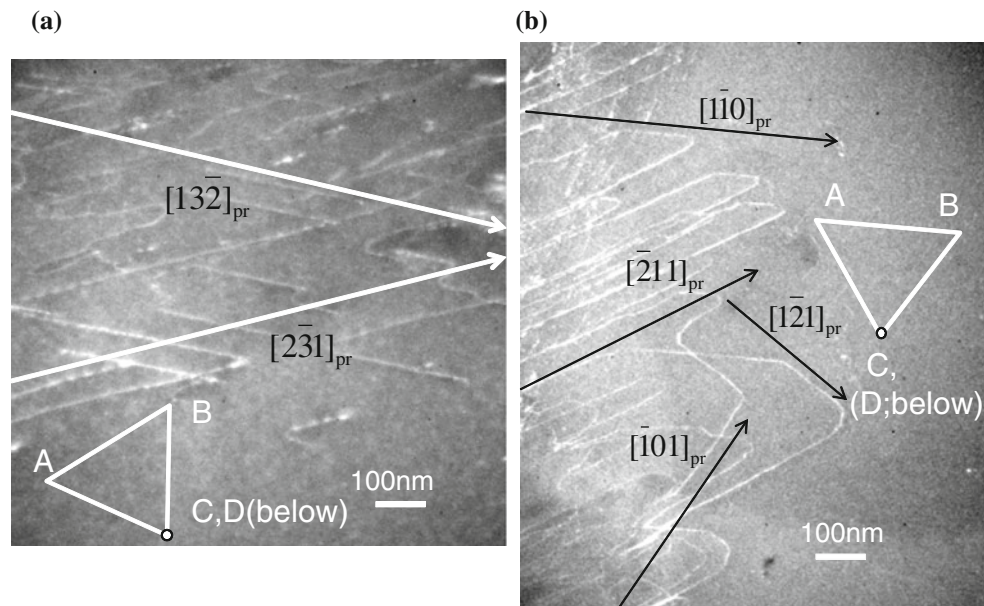


Fig. 4 Dislocations introduced at 77 K. $B = [110]$, where B is the direction of the incident beam

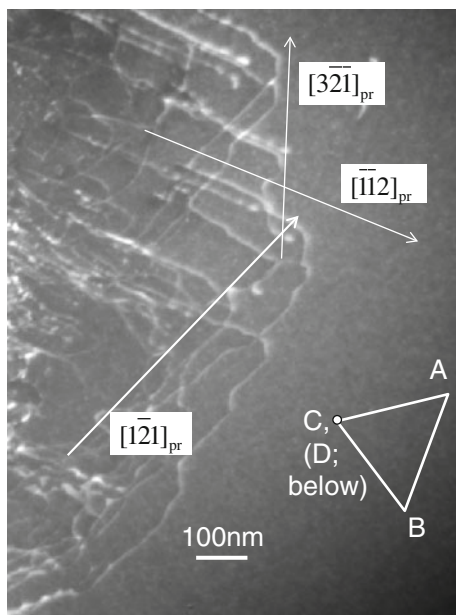


Fig. 5 Dislocations introduced at room temperature. $B = [110]$

zigzagged. In Fig. 9b, the same specimen was tilted in such a way that the dislocations are viewed end on with $B = [\bar{1}\bar{1}2]$; the dislocations are almost straight. This indicates that the zigzagged dislocations, when viewed from the top, are actually planar. Tiny wavy natures (indicated by arrows) are to be attributed to damages caused by electron bombardment during observation (this observation was carried out in a new HVEM of Nagoya University at an accelerating voltage of 1000 kV.). At 668 and 703 K, an essentially similar feature was observed.

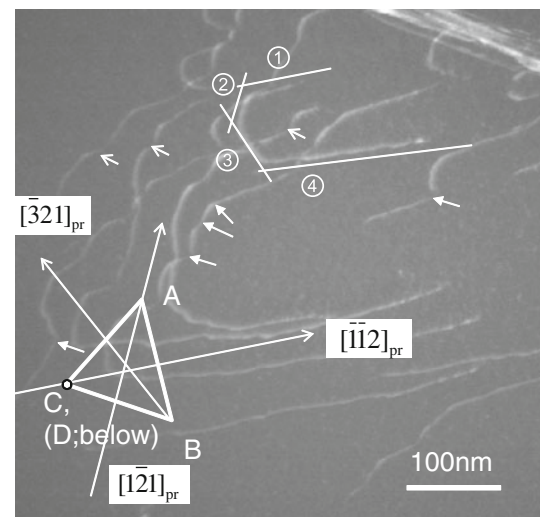


Fig. 6 Dislocations introduced at 363 K. $B = [110]$

Above 823 K

The dislocation configurations suddenly changed above 823 K. Figure 10a shows a general view, at a low magnification, of dislocations introduced at 823 K. The dislocations are either straight along $\langle 110 \rangle$ directions (indicated by A) or smoothly curved (indicated by B) without any visible cusps. Furthermore, a widely extended stacking fault such as indicated by arrow C was frequently observed.

Figure 10b shows dislocation B at a higher magnification. The dislocation is dissociated into two partials.

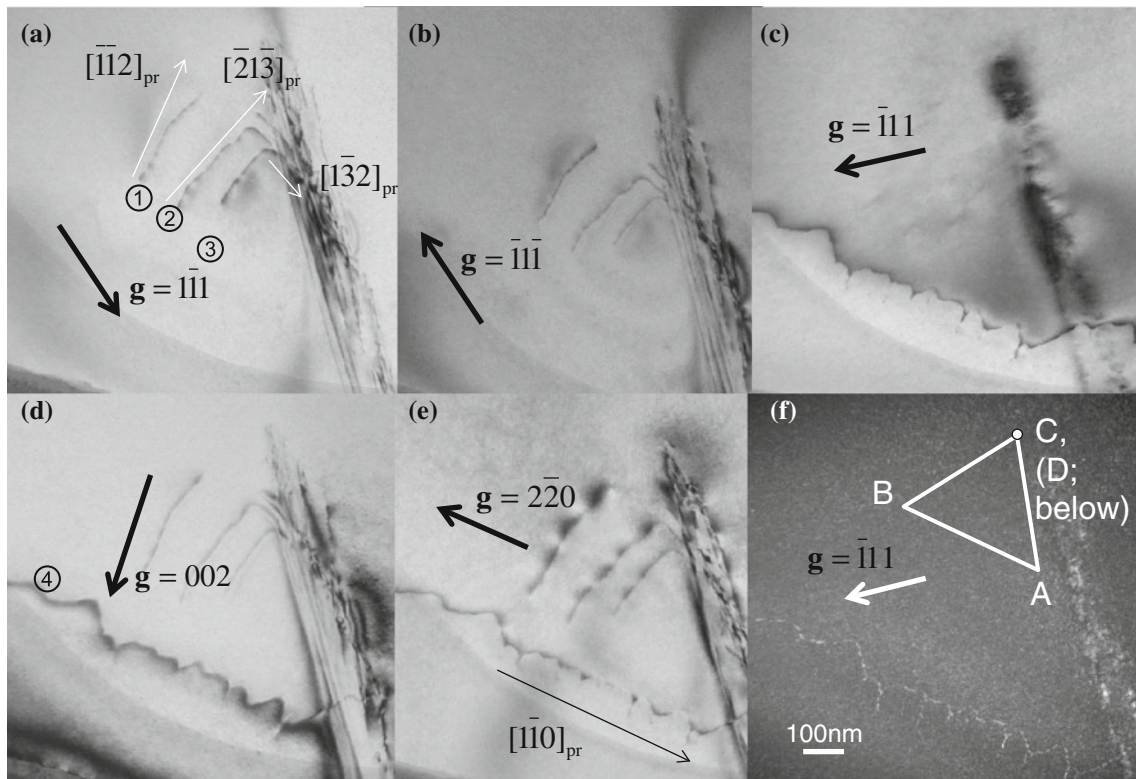


Fig. 7 Dislocations introduced at 383 K. $B = [110]$

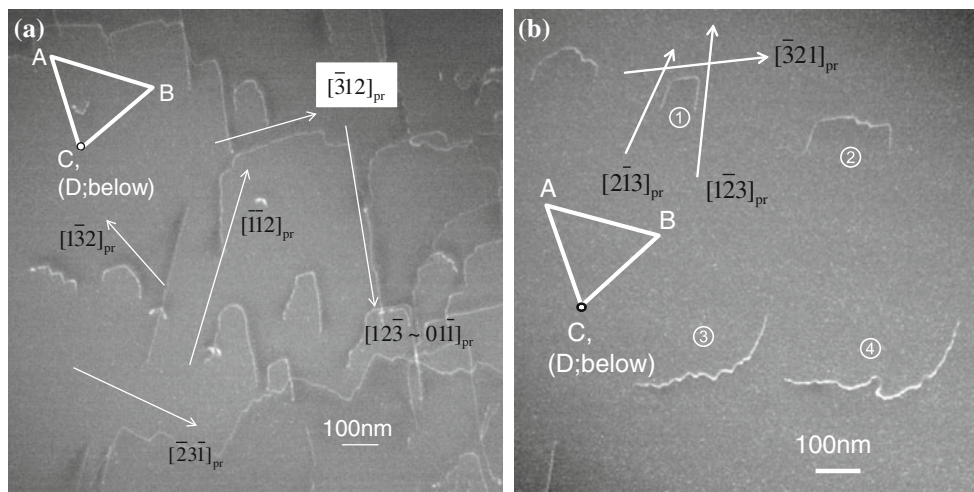


Fig. 8 Dislocations introduced at 473 K. $B = [110]$

Figure 11ab shows other examples of dissociated dislocations. Here, two dislocations ① and ② were imaged in $g = 0\bar{2}2$ (a) and $g = 02\bar{2}$ (b). Both of them show two contrasts separated by about 10 nm. In $g = 0\bar{2}2$ (Fig. 11a), the left-hand side contrast appears stronger than the right-hand side contrast. In $g = 02\bar{2}$ (Fig. 11b) the reverse is true. This contrast experiment under $\pm g$ definitely shows that these two contrasts associated with dislocations ① and ② are Shockley partials.

Possible effect of oxygen clustering

The striking feature of the dislocations in the Si described above is that the SH set of dislocations introduced at intermediate temperature (say between 363 and 703 K) is heavily zigzagged. One obvious possibility to explain this feature is that oxygen, which is contained in CZ-Si, forms clusters at this temperature range, hindering the motion of the SH set of dislocations.

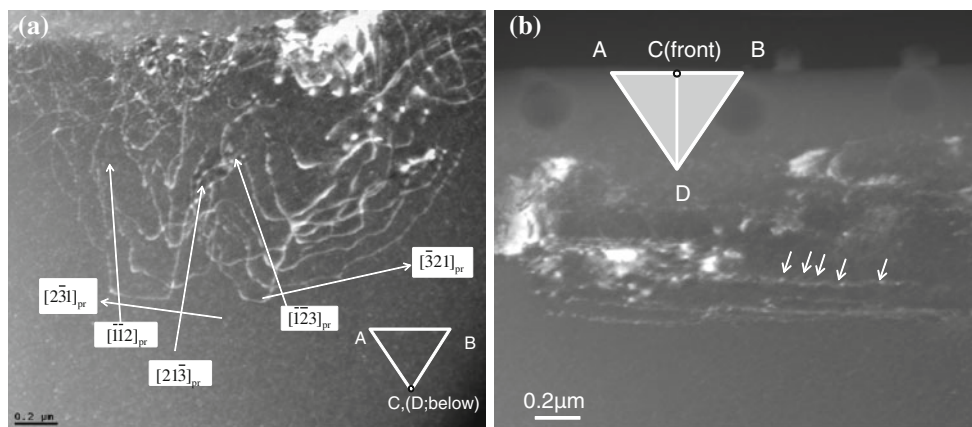


Fig. 9 Dislocations introduced at 623 K. **a** $B = [110]$, **b** $B = [11\bar{2}]$

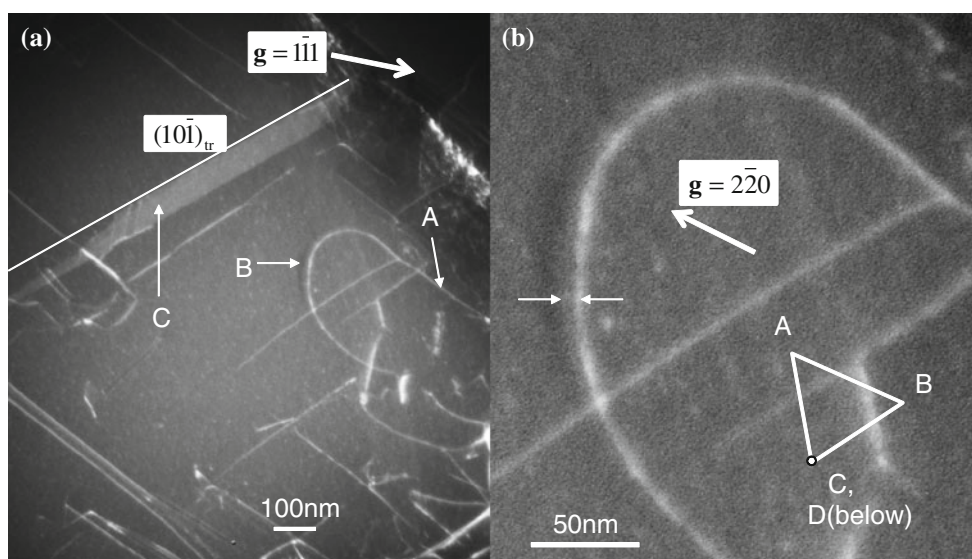


Fig. 10 Dislocations introduced at 823 K (a) at a low magnification, and (b) at a high magnification. $B = [110]$

If the zigzagged configuration is caused by clustering of oxygen contained in CZ-Si, in FZ-Si, which contains a much smaller amount of oxygen than CZ-Si, a dislocation is expected to be less zigzagged. Figure 12 shows dislocations introduced at 623 K in FZ-Si. The dislocations are zigzagged in a similar manner as in the case of CZ-Si.

Moreover, suppose that clustering takes place at the medium temperature range, say 623 K, and that this is responsible for the zigzagging of dislocations, then a dislocation introduced at low temperature (such as RT and 77 K) after a heat treatment at 623 K is to assume zigzagged configuration. On the contrary, if clustering of oxygen is not responsible for the zigzagging, a dislocation introduced at RT or 77 K after the prior heat treatment at 623 K would be straight. Figure 13 shows dislocations introduced at 77 K in CZ-Si that had been heated at 623 K

for 30 min. The dislocations are straight along $\langle 110 \rangle$ and $\langle 112 \rangle$ just as in the case of as-introduced dislocations in CZ-Si without any prior heat treatment. Thus, it is concluded that clustering of oxygen is most likely not responsible for zigzagging of the dislocations introduced in the medium temperature range.

Effect of post-annealing on dislocation configurations

The SH-GL transition temperature was estimated by comparing configurations of the as-introduced dislocations (at low temperature regime) before and after annealing at high temperature.

Figure 14 shows dislocations introduced at 77 K, followed by annealing at 573 K in the bulk form. The dislocations assume rather straight configurations lying

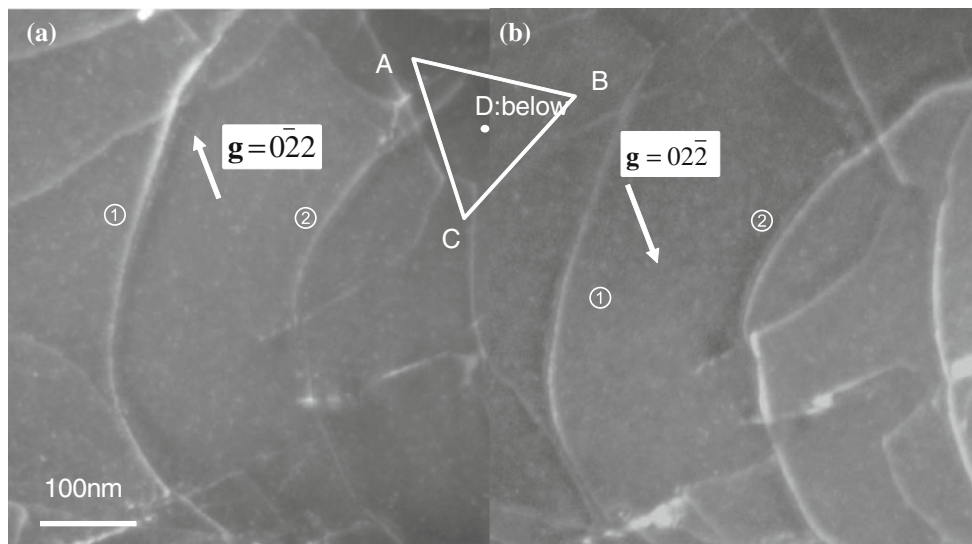


Fig. 11 Dislocations introduced at 823 K imaged in (a) $g = 0\bar{2}2$, (b) $g = 02\bar{2}$. $B = 111$. Dislocations ① and ② are dissociated into Shockley partials

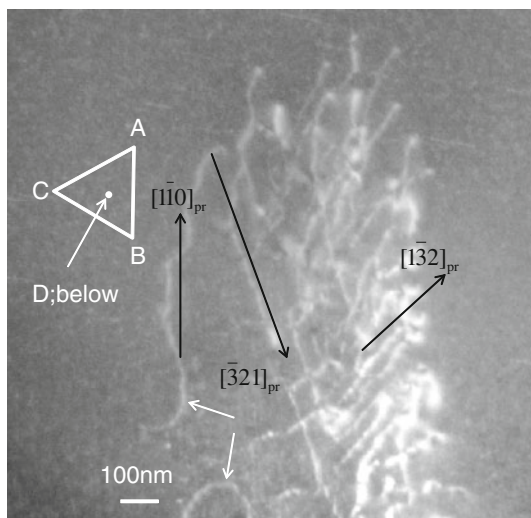


Fig. 12 Dislocations introduced in FZ-Si at 623 K. $B = [111]$

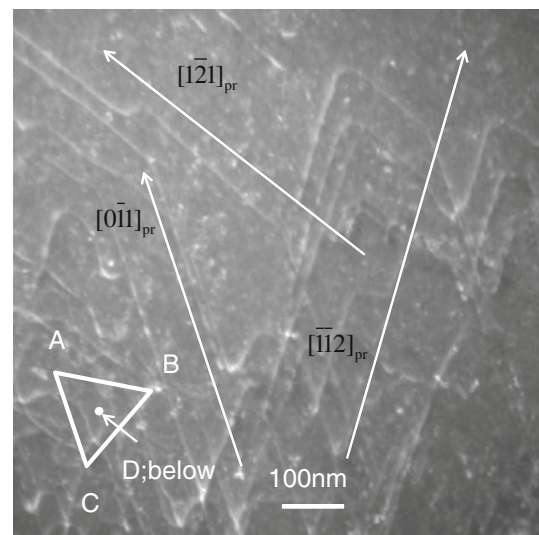


Fig. 13 Dislocations introduced at 77 K in CZ-Si that was annealed at 623 K for 30 min. $B = [111]$

approximately along $\langle 110 \rangle$ directions. This is in sharp contrast to the heavily zigzagged dislocations which were introduced at 623 K (Figs. 9a, 12). No evidence of dissociation was obtained. Thus, it is concluded that virtually no change in configuration occurred on annealing at 573 K.

In contrast to this, on annealing at 623 K, the dislocation configuration has changed completely as shown in Fig. 15. The dislocations assume hexagons and are widely dissociated, bounding the stacking fault. Thus, transition from the SH set to the GL set has occurred. This indicates that the transition temperature T_c obtained by the post-annealing method is between 573 and 623 K, about 100 K lower than the T_c estimated from the as-introduced dislocations.

Discussion

Summary of the observations

The results described above can be summarized as follows (Fig. 16). Here, the triangle indicates a very straight SH set of dislocation with sharp bends, the trapezoid indicates a rather straight (but, not so straight as the triangle) SH set of dislocation with round bends. In both cases, these SH set dislocations are parallel to $\langle 110 \rangle$, $\langle 112 \rangle$, and $\langle 123 \rangle$. The open circle indicates a heavily zigzagged SH dislocation with no particular preferred orientations. The hexagon indicates a dissociated dislocation of the GL set with hexagonal shape.

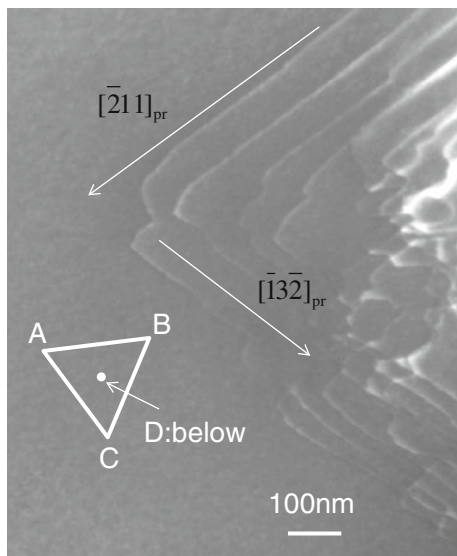


Fig. 14 Dislocations introduced at 77 K and then annealed at 573 K for 30 min in bulk state $B = [111]$

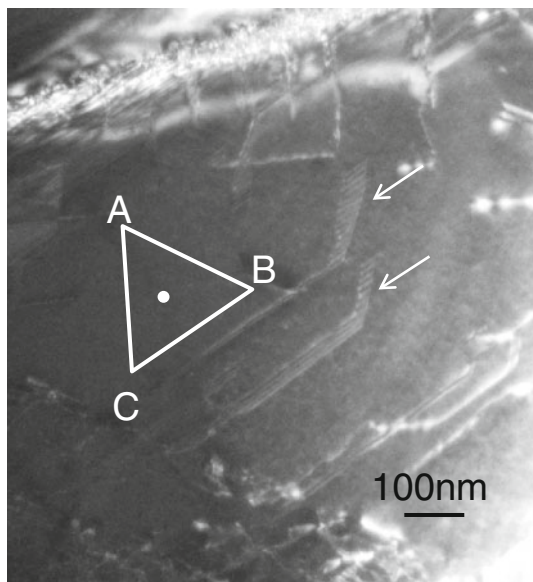


Fig. 15 Dislocations introduced at 77 K and then annealed at 623 K for 30 min in bulk state $B = [111]$

The ellipse indicates a dissociated dislocation of the GL set with smoothly curved configuration.

It is clear that there are many differences in behavior between as-introduced dislocations and annealed dislocations.

1. For the annealed dislocation, the transition from SH to GL takes place between 573 and 623 K. The SH dislocations remain very straight with sharp bends below the transition temperature ($T_{c,a}$). By contrast, for the as-introduced dislocations, the transition

temperature ($T_{c,d}$) is between 623 and 773 K, more than 100 K higher than $T_{c,a}$.

2. The configuration of the as-introduced SH dislocations take three stages, indicated by the triangle, trapezoid, and open circle in Fig. 16.

Difference in transition temperatures (T_{cd} and T_{ca})

This can be rationalized by considering the transition as a thermally activated process. In the present study, the surface of the sample was scratched at high temperatures (excepting a scratch at room temperature and 77 K), followed by immediate cooling. In this sense, the as-introduced dislocations were quenched. In the annealing experiments, the dislocations were annealed for 30 min, which may be long enough for the transformation from the SH to GL to take place. Furthermore, the strain rate in the scratching test is rather high, while during annealing, the strain rate is virtually zero. According to Samuels and Roberts [2], DBTT increases with increasing the strain rate. Thus, it is reasonable that T_{cd} (corresponding to the higher strain rate) is much higher than T_{ca} (corresponding to the lower strain rate).

Transformation in configuration of as-deformed SH dislocations

Transformation from stage I to stage II

This can be rationalized as follows:

At a very low temperature such as 77 K, the SH set of dislocations lies deep in the Peierls valleys (Fig. 17a). Thus, the dislocations are very straight and the bends are very sharp. On increasing the temperature, however, a sharp bend blunts due to the line tension (indicated by arrows in Fig. 17a) of the two dislocation lines comprising the bend. Furthermore, some segments of dislocation may overcome the Peierls potential locally due to thermal activation, leading to the formation of kinks (Fig. 17b).

The transformation from stage I to stage III

This cannot be easily explained by the line-tension mechanism, since by transforming from stage II to stage III, the total energy of a dislocation line increases. Also, the configuration of dislocations is quite heavily zigzagged; it would be difficult to consider this as being composed of short segments (kinks), each of which lies along the Peierls valley.

A novel mechanism is to be invoked to explain the transformation from stage II to stage III. For the SH set of dislocation to transform to the GL set, the SH set of

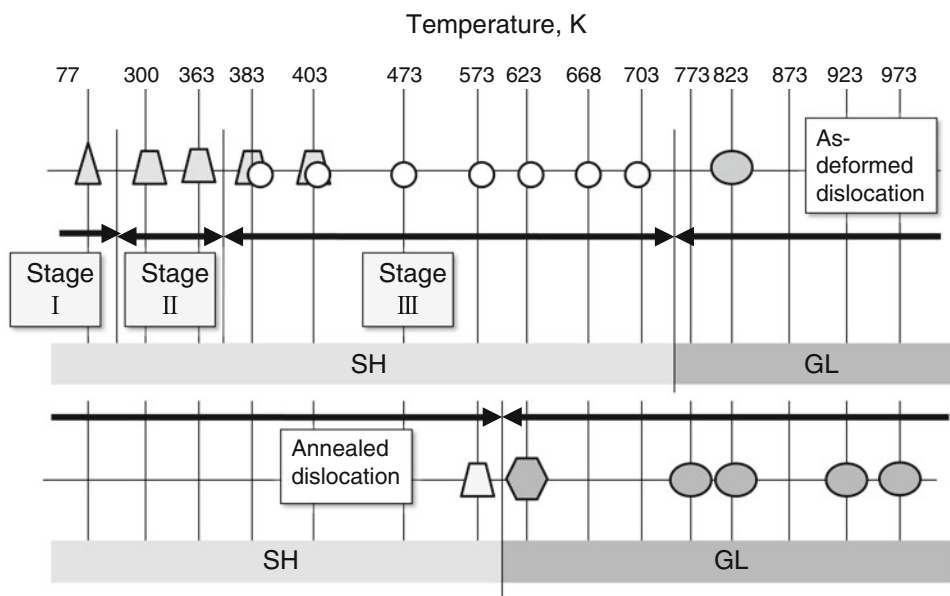


Fig. 16 Temperature dependence of the nature (GL or SH) and configuration of dislocations

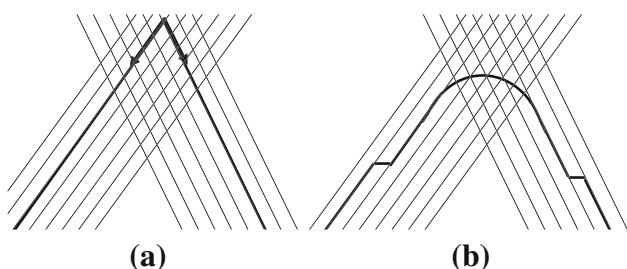


Fig. 17 Configuration of the SH dislocations in stage I(a) and II(b)

dislocation must climb by absorbing or emitting point defects or cross slip, as can be seen from Fig. 2. However, a possibility of cross slip may be eliminated for the following reason. Dislocation ④ in Fig. 7 is heavily zig-zagged. The Burgers vector of dislocation ④ is parallel to BC. Suppose this dislocation was originally straight, then dislocation ④ is initially a 60° dislocation and not a screw dislocation. If cross slip is responsible for the local transformation from the SH to GL dislocation, zigzagging is not expected to occur along dislocation ④, which is not a screw dislocation initially. Thus, the only possible mechanism responsible for the transformation is climb.

In the case depicted in Fig. 2a, the SH of dislocation must climb up from A'B'C' (d') to ABC (d). The equilibrium concentration of point defects such as vacancy increases with increasing temperature. Suppose that, at a moderately high temperature, the SH set of dislocation (the Burgers vector of which is, say, A'C') absorbs vacancies and climbs to transform segments of the GL set. In other words, the dislocation, initially having the Burgers vector

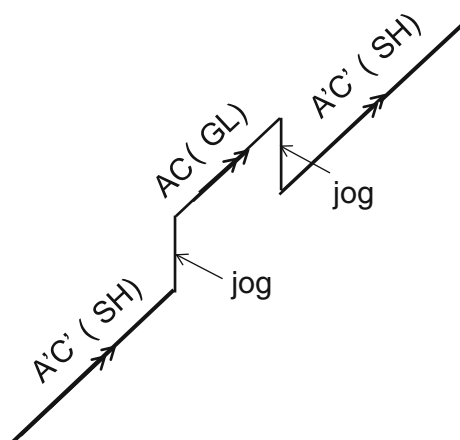


Fig. 18 Transformation of the SH dislocation from stage II to III

A'C', is now composed of segments with A'C' and AC (Fig. 18).

There are two possibilities.

1. The GL set of dislocations is more mobile.
2. The SH set of dislocations is more mobile.

In the case of (1), the GL set of dislocation segments bows out, leaving the SH segments behind. In the case of (2), the reverse is true. Experimental results obtained in the present study show definitely that case (2) is true. Here, it is assumed that the associated jogs are immobile. The detailed structure of the jogs is unknown, which is hoped to be studied in future.

The aforementioned discussion leads to the following conclusion.

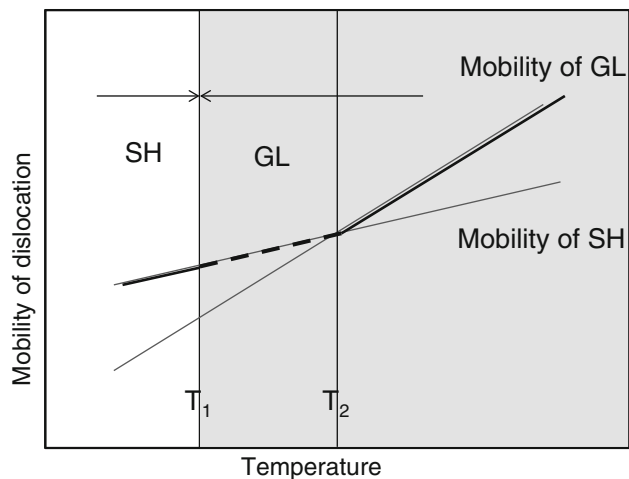


Fig. 19 Stability and mobility of the GL and SH dislocations as functions of temperature. Mobility of the GL and SH dislocations crosses over at T_2 . Stability of the GL and SH dislocations crosses over at T_1 , which most probably depends on the strain rate in such a way that T_1 increases with increasing the strain rate

Mobility of the GL set and SH set of dislocations increases with increasing temperature as shown in Fig. 19. Below T_2 , the SH set of dislocations is more mobile than the GL set of dislocations, as is well accepted. T_2 is to correspond to the DBTT. However, even below T_2 , the SH set of dislocations can transform to the GL set of dislocations if the temperature is higher than another critical temperature T_1 , where the concentration of vacancy is high enough. These segments of the GL set are less mobile than the remaining dislocation of the SH set. In other words, between T_1 and T_2 , the GL set of dislocation segments plays a role of pinning points for the motion of the SH set of dislocations. This is the reason why the SH set of dislocations is so heavily zigzagged in the intermediate temperature.

It must be mentioned that in the present study, no evidence was obtained for the dissociation at sharp bends on the SH dislocations. Korte et al. [14] observed a “weakly dissociated dislocation” at 373 K, which is close to the lower limit of the stage II in the present study. The reason for this difference is not clear and a more detailed study is hoped to be carried out to clarify the reason.

Conclusion

It has been shown that just below the DBTT, the SH set of dislocations is heavily zigzagged, and this is attributed to

the mixture of the SH set and the GL set of dislocations. In other words, in this temperature range, the GL set of dislocations has lower energy than the SH set of dislocations, while the mobility of the GL set of dislocations is still lower than that of SH set of dislocations. As a result, the dislocations (mostly of the SH set) are heavily zigzagged.

Such a mixture of dislocations with different natures (or configuration) usually leads to the reverse temperature dependence of the strength, as in the case of $L1_2$ [17] and B2 ordered alloys [18]. Thus, such a reverse temperature dependence of the strength may be expected for Si.

Acknowledgements The authors thank Dr. S.Arai and Mr. T.Suzuki for assistance in operating high-voltage electron microscopes. The authors also thank Ms.Y. Yoshikawa for advice in preparing thin foil specimens by FIB. H. S thanks the Ministry of Education, Culture, Sports, Science and Technology for the financial support (Grant-in-Aid for Scientific Research (C), Contract #24560803).

References

- Hirth JP, Lothe J (1982) Theory of Dislocations. Wiley, New York
- Samuels J, Roberts SG (1989) Proc Roy Soc Lond A421:1–23
- Cockayne DJH, Ray ILF, Whelan MJ (1969) Philos Mag 20:1265–1270
- Gomez A, Cockayne DJF, Hirsch PB, Vitek V (1975) Philos Mag 31:105
- Wessel K, Alexander H (1977) Philos Mag 35:1523–1536
- Hill MJ, Rowcliffe DJ (1974) J Mater Sci 9:1569–1576
- Rabier J, Denantot F, Dement JL, Cordier P (2004) Mater Sci Eng A387–389:124–128
- Rabier J, Cordier P, Dement JL, Garem H (2001) Mater Sci Eng A 309–310:74–77
- Rabier J, Pizzagalli L, Dement JL (2010) Dislocations in silicon at high stress. In: Hirth JP, Kubin L (eds) Dislocations in solids, vol 16. Elsevier, Amsterdam, p 47
- Asaoka K, Umeda T, Arai S et al (2005) Mater Sci Eng A 400–401:93–96
- Saka H, Yamamoto K, Arai S et al (2006) Philos Mag 86:4841–4850
- Nakao S, Ando T, Shikida M et al (2008) J Micromech Microeng 18:Article # 015026
- Izumi S, Ohta H, Takahashi C et al (2010) Philos Mag Lett 90:707–714
- Korte S, Barnard JS et al (2011) Int J Plast 27:1853–1866
- Rabier J, Cordier P, Tonedellier T et al (2000) Condens Matter 12:10059–10064
- Tanaka N et al (2010) Proceeding of IMC,IFSM, Aptom Software 19_2 ISBN: 978-85-63273-06-2
- Vitek V, Pope D P, Bassani JL (1996) In: Nabarro FRN (ed) Dislocations in solids, vol 10. North-Holland, Amsterdam, p 135
- Caillard D, Couret A (1996) In: Nabarro FRN (ed) Dislocations in solids, vol 10. North-Holland, Amsterdam, p 69